

# Thermal Chemistry of 1,6-Diiodohexane on Ni(100) Single-Crystal Surfaces: Mimicking Cyclization Reactions

Sariwan Tjandra and Francisco Zaera\*

Department of Chemistry, University of California, Riverside, California 92521

Received: September 16, 1998; In Final Form: November 20, 1998

The thermal chemistry of 1,6-diiodohexane, 6-bromo-1-hexene, 1,5-hexadiene, methyl cyclopentane, methylene cyclopentane, and 1-methyl-1-cyclopentene on Ni(100) surfaces has been studied under ultrahigh vacuum conditions by X-ray photoelectron spectroscopy (XPS) and temperature-programmed desorption (TPD). The thermal activation of the diiodo alkane leads to the initial scission of the C–I bonds around 160 K, the same as with other iodoalkanes, and presumably results in the formation of a surface metallacyclic intermediate. Further heating of that system induces the desorption of hexene, hexane, iodohexane, methylene cyclopentane, benzene, and cyclohexene. The formation of the latter two cyclic products through 5-hexen-1-yl, methyl cyclopentane, methylene cyclopentane, or 1-methyl-1-cyclopentene intermediates was ruled out in this case because direct activation of those compounds does not lead to the desorption of any C<sub>6</sub>-cyclic molecules at all. TPD experiments with 1,5-hexadiene, on the other hand, did show the formation of benzene, suggesting that such a molecule could be involved in the conversion of the diiodohexane. Additional results from studies with cyclohexane, iodocyclohexane, and cyclohexene indicate that the first cyclic intermediate from the reaction of the C<sub>6</sub>–Ni metallacycle is likely to be cyclohexene, since both cyclohexane and cyclohexyl moieties yield much more cyclohexane than the diiodo compound. On the basis of these data, a mechanism is proposed for the cyclization reaction of nickelacycloheptane where two initial  $\beta$ -hydride elimination steps at both ends of the hydrocarbon moiety result in the formation of adsorbed 1,5-hexadiene and where that is followed by insertion of one of the double bonds into the metal–carbon bond at the other end to yield cyclohexene.

## 1. Introduction

The catalytic cyclization of alkanes to cycloalkanes and aromatics is of significant practical importance in industry, particularly in connection with petroleum reforming.<sup>1–3</sup> One of the key factors in determining the usefulness of a given catalyst for this type of reaction is its ability to promote cyclization steps selectively, that is, at the expense of other undesirable pathways such as hydrogenolysis. Particularly puzzling is the fact that among transition metals only platinum appear to be able to do this well; nickel, for instance, excels in aiding C–C bond-breaking steps instead. On the basis of recent surface-science experiments, we have argued that the difference in catalytic selectivity between nickel and platinum may be the intrinsic ability of the former to readily induce multiple dehydrogenation steps at the a carbon of the initial alkyl surface intermediates (the one directly bonded to the metal).<sup>4,5</sup> Nevertheless, much more work is needed to pin down the relative rates of the several reaction pathways available to hydrocarbons on different transition metal surfaces before a complete microscopic picture of the fundamental factors involved in the designing of reforming catalysts can be developed. In this paper, we report research done by us to probe the mechanism of cyclization reactions on Ni(100).

Although past experiments with simple iodoalkanes had never provided evidence for C–C coupling steps on nickel surfaces,<sup>6–11</sup> the ability of that metal to promote the production of cyclic hydrocarbons was demonstrated recently in experiments with dihalopropanes.<sup>12</sup> Specifically, the thermal activation of either

1,3-diiodopropane or 1-chloro-3-iodopropane leads to the evolution of cyclopropane, presumably via the formation of a nickelacyclobutane intermediate. Since cyclization reactions are expected to occur more easily with alkanes large enough to generate five- or six-membered ring structures, we turned our interest to the exploration of the chemistry of 1,6-diiodohexane. Evidence from catalytic studies has shown that indeed cyclization and isomerization processes usually involve C<sub>5</sub> or C<sub>6</sub> intermediates.<sup>13</sup> The results reported here prove that such cyclization steps can be induced on nickel under vacuum conditions as well, but that they do not appear to follow the mechanism commonly proposed in the catalysis literature. In particular, it was found that the thermal conversion of 1,6-diiodohexane on Ni(100) is dominated by the direct formation of cyclohexene, without the involvement of any C<sub>5</sub> (methyl cyclopentane, methylene cyclopentane, or 1-methyl-1-cyclopentene) or 5-hexen-1-yl intermediates. Experiments with other C<sub>6</sub>-cyclic hydrocarbon precursors led to the proposal of a mechanism where the initial metallacyclic surface moiety first undergoes  $\beta$ -hydride elimination steps at both ends of the chain to yield adsorbed 1,5-hexadiene, after which one of the double bonds of this hexadiene inserts into a metal–carbon bond at the other end to produce cyclohexene.

## 2. Experimental Section

The experiments reported here were carried out in an ultrahigh vacuum (UHV) apparatus described in previous publications.<sup>14–16</sup> Briefly, the UHV chamber is evacuated by a turbomolecular pump to a base pressure of less than  $1 \times 10^{-10}$  Torr and is equipped with instrumentation for temperature-programmed

\* Corresponding author.

desorption (TPD), X-ray photoelectron (XPS), static secondary ion mass (SSIMS), Auger electron (AES), and ion scattering (ISS) spectroscopies. The quadrupole mass spectrometer used for TPD is capable of detecting masses in the 1–800 amu range, and has its ionizer located inside an enclosed compartment with 7 mm diameter apertures in its front and back for gas sampling and exit to the quadrupole rods, respectively. The sample is positioned within 1 mm of the front aperture in order to selectively detect the molecules that desorb from the front face of the crystal. The mass spectrometer is interfaced to a computer in order to acquire the signal for up to 15 different masses simultaneously in a single desorption experiment. Specific amu's were selected here to represent the different species in the TPD experiments, but the identity of the desorbing compounds was always corroborated by following the signal of other key masses in their cracking pattern. Also, the TPD traces reported in this paper correspond to the raw data for the indicated amu's, except for the cases of the cyclohexene and cyclohexane spectra from 1,6-diiodohexane presented in Figure 9, where the contributions from methylene cyclopentane, hexene, and molecular desorption were removed from the 82 and 84 amu traces by a deconvolution procedure described in previous publications.<sup>17,18</sup> The TPD signals are in reported arbitrary units, but their intensities are referred to the same standard given by the scale bar shown at the top of each figure. A heating rate of about 10 K/s was used in these TPD runs. XPS spectra were taken by using an Al anode and a hemispherical electron energy analyzer with an overall energy resolution of about 1.2 eV full width at half-maximum. The binding energy scale was calibrated against those of the Pt 4f<sub>7/2</sub> and Cu 2p<sub>3/2</sub> photoelectrons.

The nickel single crystal was cut and polished in the (100) orientation using standard procedures and spot-welded to two tantalum rods attached to a manipulator capable of cooling to liquid-nitrogen temperatures and resistively heating to above 1500 K. The crystal temperature was monitored with a chromel–alumel thermocouple spot welded to the edge of the crystal. Cleaning of the surface by cycles of oxygen treatment, ion sputtering, and annealing was done prior to each experiment until no impurities were detected by either Auger electron or X-ray photoelectron spectroscopies. The organic compounds were all purchased from Aldrich (97–99% purity) and subjected to several freeze–pump–thaw cycles before being introduced into the vacuum chamber; their purity was checked periodically by mass spectrometry. Gas doses are reported in langmuirs (1 langmuir =  $1 \times 10^{-6}$  Torr) and are not corrected for differences in ion gauge sensitivities.

### 3. Results

The thermal conversion of 1,6-diiodohexane (IC<sub>6</sub>H<sub>12</sub>I) was studied first by using X-ray photoelectron spectroscopy and temperature-programmed desorption. The iodine 3d XPS spectra (not shown) displayed the red shift around 160 K characteristic of the rupture of C–I bonds seen in other adsorbed alkyl iodides.<sup>6,11,14,19</sup> Unfortunately, the I 3d photoelectron signal overlaps with that from the Ni LVV Auger electrons and is too weak in this case to allow for any detailed study of the C–I bond-scission steps in 1,6-diiodohexane. Specifically, it could not be determined conclusively if those bonds break sequentially or simultaneously. Nevertheless, indirect evidence from the TPD experiments as well as previous results from the study of dihalopropanes on Ni(100)<sup>12</sup> strongly supports the former hypothesis. In any case, no C–I bonds remain intact on the surface above 160 K. There is a significant reduction in iodine coverage on the surface upon heating to 160 K, presumably

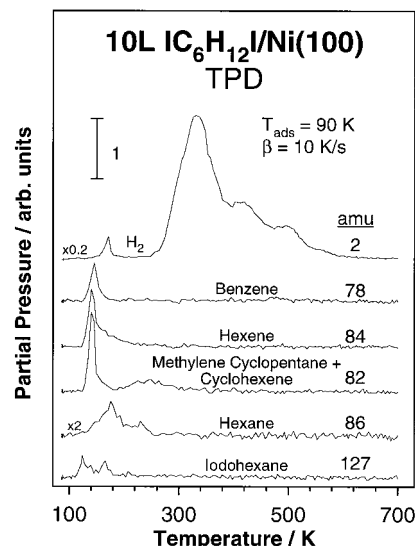


**Figure 1.** 2 (hydrogen), 78 (benzene), 84 (hexene), 82 (cyclohexene and methylene cyclohexane), 86 (hexane), and 127 (iodohexane) amu temperature-programmed desorption (TPD) spectra from Ni(100) surfaces dosed with 10.0 langmuirs of 1,6-diiodohexane at 90 K. A heating rate of 10 K/s was used in all the TPD experiments reported here (L = langmuir).

because of the desorption of iodohexane (see below). The saturation coverage of the diiodo compound (the amount that decomposes on the surface) was grossly estimated to be about 0.1–0.2 ML.

Figure 1 shows TPD spectra obtained after the adsorption of 10.0 langmuirs of 1,6-diiodohexane (an exposure slightly below that needed for monolayer saturation) on Ni(100) at 90 K. In addition to hydrogen, at least six different hydrocarbons were seen to desorb from that surface, namely, iodohexane, hexane, cyclohexene, methylene cyclopentane, hexene, and benzene. Many other possible products were checked but not detected, including methyl cyclopentane, methyl cyclopentene, cyclohexane, cyclohexadiene, and hexadiene (although the evidence against the formation of the last is not compelling). Iodohexane, which was followed by the signal for 127 amu, must form via the hydrogenation of 6-iodo hexyl moieties (the product from scission of only one of the C–I bonds in the diiodohexane) and desorbs in a broad temperature range between 120 and 180 K. The main desorption features for hexene and hexane are seen at 140 and 175 K, respectively; by using Redhead's equation<sup>20</sup> and a preexponential factor of  $1 \times 10^{13} \text{ s}^{-1}$ , activation energies of about 8.0 and 10.1 kcal/mol are estimated for the desorption of those two species. Benzene production is seen as a reasonably sharp feature peaked at 145 K. Hydrogen evolves in a main peak at 330 K and two shoulders at 415 and 490 K.

The interpretation of the information from the 82 amu TPD trace is complicated by the significant overlap of signals from several possible C<sub>6</sub> hydrocarbons, and requires further analysis via a comparison with the mass fragmentation pattern of the corresponding potential products. To illustrate the procedure used in this work to solve this problem, the mainframe of Figure 2 shows the 54, 67, and 82 amu traces recorded for the TPD from 10.0 langmuirs of 1,6-diiodohexane on Ni(100), and the inset compares their relative intensities to those from the mass spectra of the pure compounds of the most likely products with a 82 amu parent peak, namely, 1,5-hexadiene (Diene), cyclohexene (C-Hex), methylene cyclopentane (CH<sub>2</sub>-C5), and 1-methyl-1-cyclopentene (CH<sub>3</sub>-C5). It can be seen in that figure that the match between the cracking pattern of the first two peaks of the diiodohexane TPD and that of cyclohexene is excellent,

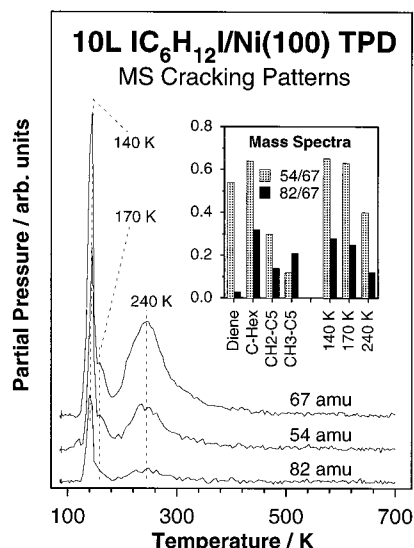


**Figure 2.** Comparison between the 67, 54 and 82 amu traces from TPD experiments with 10.0 langmuirs of 1,6-diiodohexane on Ni(100) (mainframe) and the mass spectrometry cracking pattern from gaseous 1,5-hexadiene (Diene), cyclohexene (C-Hex), methylene cyclopentane (CH<sub>2</sub>-C5) and 1-methyl-1-cyclopentene (CH<sub>3</sub>-C5) obtained under the same experimental conditions (inset). These data allowed for the identification of the species desorbing at 140 and 170 K as cyclohexene and that at 240 K as methylene cyclopentane (L = langmuir).

**TABLE 1: Comparison of the Mass Spectrometer Cracking Patterns for 1-Hexene, Cyclohexene, and Methyl Cyclopentane with Those for the Products That Desorb from Thermal Activation of 1,6-Diiodohexane on Ni(100) (a Clear Match Is Seen with the Hexene)**

amu	mass spectra			TPD
	1-hexene	cyclohexene	methyl cyclopentane	1,6-diiodohexane (140 K peak)
56	100	100	100	100
84	34	74	13	36

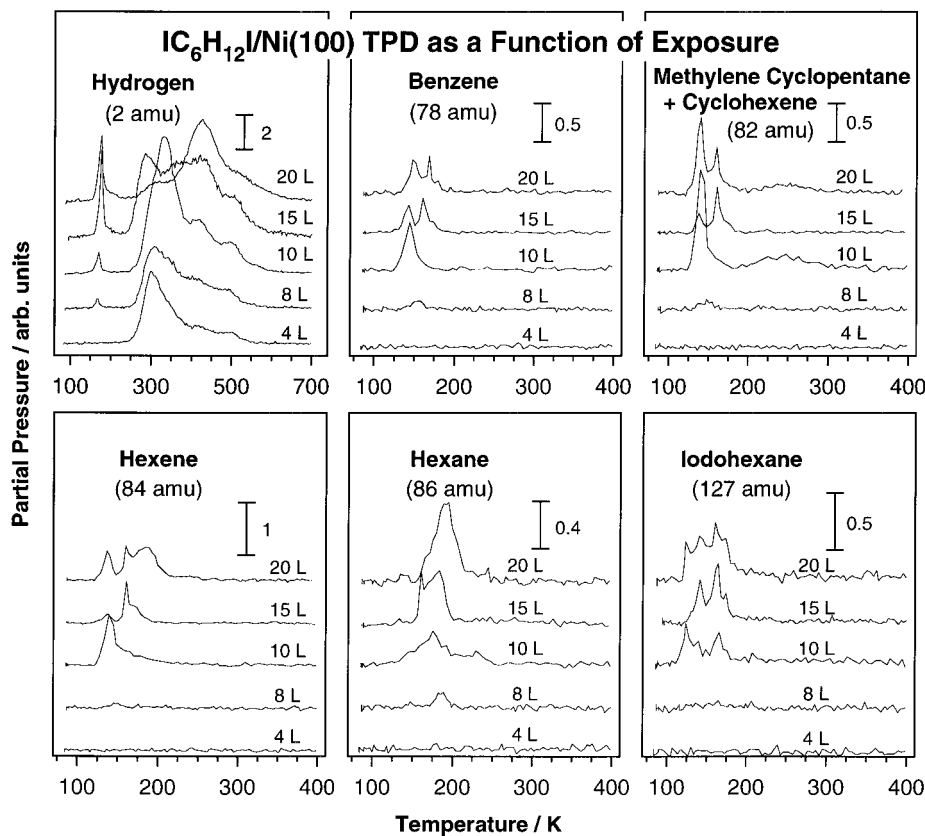
implying that that is the molecule that desorbs at 140 and 170 K. Although the agreement is not as good for the 240 K feature, it seems quite reasonable to assign it to methylene cyclopentane. A similar analysis with the 84 amu peak and its main fragment at 56 amu indicated that the TPD data for those masses from 1,6-diiodohexane most likely corresponds to 1-hexene, and ruled out both cyclohexene and methyl cyclopentane as possible products in this system (Table 1).

A more careful TPD study of the evolution of hydrogen, benzene, cyclohexene, methylene cyclopentane, hexene, hexane, and iodohexane from 1,6-diiodohexane decomposition as a function of initial coverage is shown in Figure 3. The H<sub>2</sub> TPD traces (Figure 3a) indicate that after a 4.0 langmuir exposure most of the hydrogen desorption occurs around 300 K, even though there are two small shoulders about 415 and 490 K as well. As the 1,6-diiodohexane exposure is increased, the main feature grows and shifts toward higher temperatures, to 335 K for a 10.0 langmuir exposure, but the relative shape of the whole trace remains approximately the same. However, after coverages beyond 10.0 langmuirs, the desorption intensity below 350 K decreases significantly and the spectra becomes dominated by the features at 430 and 500 K, which retain approximately the same shape as in the lower exposures. This evolution indicates that the early extensive dehydrogenation that occurs at low coverages is severely inhibited as the surface becomes crowded, at which point the hydrocarbon surface moieties survive until relatively high temperatures.

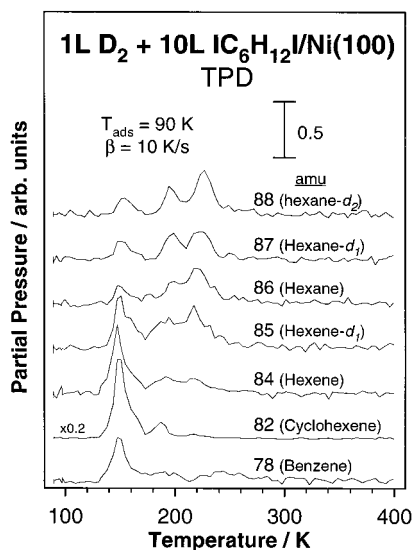
Figure 3b displays the benzene (78 amu) TPD spectra obtained from 1,6-diiodohexane adsorbed on Ni(100) as a function of initial exposure. Benzene desorption starts only after a dose of 8.0 langmuirs, initially as one single peak about 145 K (which corresponds to an activation energy of about 8.4 kcal/mol) and later in an additional sharp feature that grows at 165 K for initial exposures of the iodide above 10.0 langmuirs. Figure 3c summarizes the coverage dependence of the cyclohexene and methylene cyclopentane (82 amu) TPD spectra. Again, no signal is seen here for 1,6-diiodohexane doses below 8.0 langmuirs, but a small amount of cyclohexene begins to desorb about 145 K after 8.0 langmuirs. That peak grows significantly as the dose is increased by another 2.0 langmuirs (to 10.0 langmuirs), at which point a second feature develops at about 170 K. A third broad peak appears around 240 K after the 10.0 langmuir exposure corresponding to the desorption of methylene cyclopentane. The estimated activation barriers for the desorption of cyclohexene and methylene cyclopentane in these spectra are about 8.4 and 14.0 kcal/mol, respectively.

Figure 3d shows the hexene (84 amu) TPD spectra obtained as a function of 1,6-diiodohexane exposure on Ni(100). Desorption in this case starts at an exposure of 10.0 langmuirs and is first seen at 140 K. Increasing the 1,6-diiodohexane exposure further results in a change in peak shape and in the evolution of additional features around 160 and 185 K. Figure 3e, which summarize the coverage dependence of the hexane (86 amu) TPD traces, indicates an initial desorption around 185 K at 8.0 langmuirs; larger doses lead to the growth and broadening of that desorption feature. Finally, iodohexane is also produced after exposures of 10.0 langmuirs or more, and desorbs between approximately 120 and 170 K, a temperature range about 50 K lower than that seen for the molecular desorption of 1-iodohexane adsorbed on Ni(100).<sup>11</sup>

The peak multiplicity and broad nature of the TPD traces for the hydrocarbon products detected in TPD experiments with 1,6-diiodohexane on Ni(100) suggest a complex mechanism for the conversion of the species that form on the surface. To probe those steps in more detail, additional TPD experiments were performed on surfaces predosed with either hydrogen or deuterium. Figure 4 displays an example of the data obtained from those studies, in this case for a 1.0 langmuir D<sub>2</sub> dose followed by a 10.0 langmuir diiodohexane exposure. The results from those experiments suggest that cyclization steps are unaffected by the presence of deuterium (hydrogen) atoms on the surface, since the traces for benzene and cyclohexene in this case resemble quite closely those obtained on the clean nickel surface (compare the data for the 78 and 82 amu in Figures 1 and 4). The spectrum for hexene evolution (84 amu) also looks similar to that from the experiment without deuterium coadsorption, except that a new weak and broad feature develops between 180 and 250 K, indicating that dehydrogenation ( $\beta$ -hydride elimination in particular) is facile on hydrogen-(deuterium-) precovered surfaces as well. The interesting observation from these studies is the fact that not only is there an increase in yield for hydrogenation products such as hexene and hexane in the presence of surface deuterium, but that multiple deuterium labeling takes place to a significant extent as well. For one, hexene-*d*<sub>1</sub> is produced in two stages, around 150 and 200 K; notice that the later feature is new, since no hexene evolves at such high temperatures in experiments with diiodohexane on the clean surface. In addition, the production of hexane with zero, one, and two deuterium substitutions is seen in several temperature stages around 150, 195, and 225 K. Hexane-*d*<sub>2</sub> is the product expected from double deuteration



**Figure 3.** Hydrogen (2 amu, left top panel), benzene (78 amu, top center), cyclohexene and methylene cyclopentane (82 amu, top right), hexene (84 amu, bottom left), hexane (86 amu, bottom center), and iodohexane (127 amu, bottom right) TPD spectra from 1,6-diiodohexane adsorbed on Ni(100) as a function of initial exposure. The dosing was done at 90 K in all cases (L = langmuir).



**Figure 4.** 78 (benzene), 82 (cyclohexene), 84 (hexene), 85 (hexene- $d_1$ ), 86 (hexane), 87 (hexane- $d_1$ ), and 88 (hexane- $d_2$ ) amu TPD from 10.0 langmuirs of 1,6-diiodohexane dosed on a Ni(100) pre-dosed with 1.0 langmuir of  $D_2$ . All dosings were done at 90 K (L = langmuir).

of the metallacycle intermediate that forms after activation of both C–I bonds in adsorbed diiodohexane.

The purpose of this work was to probe cyclization reactions, which in the 1,6-diiodohexane/Ni(100) system are manifested by the production of cyclohexene and benzene. The next step in our investigation was the search of possible surface intermediates for such reactions. First, to test whether a 5-hexen-1-yl species is an intermediate in the formation of cyclic hydrocarbons from 1,6-diiodohexane, some XPS and TPD

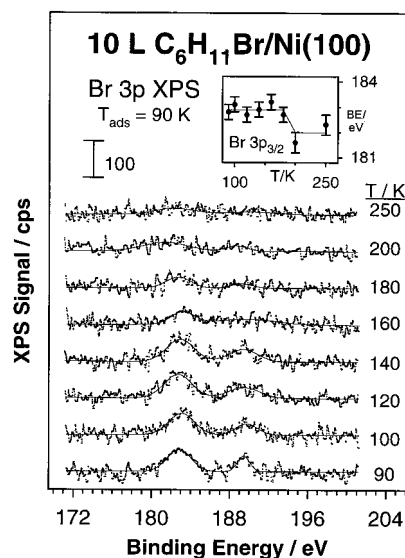


**Figure 5.** Br 3p X-ray photoelectron spectra (XPS) from a Ni(100) surface exposed to 10.0 langmuirs of 6-bromo-1-hexene at 90 K as a function of annealing temperature. The dots are the raw data, while the lines are the best fits to Gaussian peaks. The inset, which displays the position of the Br  $3p_{3/2}$  feature as a function of temperature, highlights the shift around 200 K associated with the scission of the C–Br bond (L = langmuir).

experiments were performed with 6-bromo-1-hexene on Ni(100); thermal dissociation of the C–Br bond of that precursor is expected to lead to the formation of the desired 5-hexen-1-yl moieties. Figure 5 shows that there is a shift in the Br  $3p_{3/2}$  XPS signal around 200 K, from about  $182.8 \pm 0.2$  eV to approximately 182.0 eV, indicating that indeed the C–Br bond-scission step occurs below that temperature. There is also a

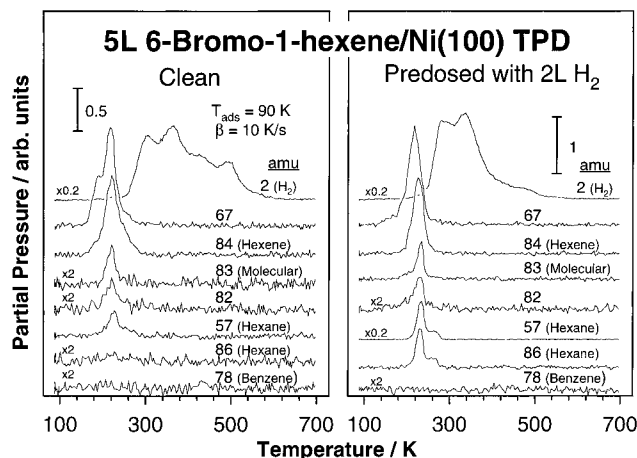


**Figure 6.** 2 (hydrogen), 67 (hexadiene and bromohexene), 84 (hexene), 83 and 82 (molecular desorption), 57 and 86 (hexane), and 78 (benzene) amu TPD from 5.0 langmuirs of 6-bromo-1-hexene dosed on clean (left) and 2.0 langmuirs  $H_2$ -predosed (right) Ni(100) surfaces. No benzene was ever detected in experiments with this molecule ( $L =$  langmuir).

significant reduction in the XPS signal intensity around 160 K indicative of the desorption of over half of the bromine-containing molecules, most likely in the form of bromohexane.

The thermal chemistry of 5-hexen-1-yl was probed further by TPD. The left panel of Figure 6 shows the data obtained from 5.0 langmuirs of 6-bromo-1-hexene on a clean Ni(100) surface. The main desorbing product in this case is the hydrogen that results from dehydrogenation of the surface species; several features are seen in the  $H_2$  TPD trace at about 300, 365, 420, and 485 K. Some hexene (84 amu) is produced around 220 K, most likely via the reductive elimination of the hexenyl species with surface hydrogen, and a small amount of hexane (57 and 86 amu) is also detected from hydrogenation of the hexene about 228 K. The remaining traces are a bit more difficult to interpret. First, the relative ratio of the signals for 82 and 83 amu suggests that those are mainly due to molecular 6-bromo-1-hexene desorption, although the trace for 82 amu may contain contributions from other species (methylene cyclopentane in particular). Second, the trace for 67 amu displays two features, the first of which corresponds to hexadiene (the shoulder at 190 K); the peak at 215 K includes some signal from molecular desorption but may also originate in part from some methylene cyclopentane desorption. What seems clear from these TPD of 6-bromo-1-hexene on clean nickel is the fact that no  $C_6$ -cyclic hydrocarbons, either cyclohexene or benzene, are produced in detectable amounts, thus suggesting that the formation of those compounds in the case of 1,6-diiodohexane does not proceed through a hexenyl intermediate.

The right panel of Figure 6 displays TPD results from an experiment where the Ni(100) surface was dosed with 2.0 langmuirs of hydrogen prior to the 5.0 langmuir exposure to 6-bromo-1-hexene. As for the case of the clean surface, some hexene is produced at 225 K in approximately the same yield. A bit more molecular desorption is observed, as indicated by the doubling of the 83 amu peak intensity, and the production of both hexadiene and methylene cyclopentane is almost completely inhibited (the signal in the 67 amu trace can be accounted for exclusively by molecular desorption). The most noticeable change, however, is the significant (about 10-fold) increase in the formation of hexane, which now shows up clearly in the 57 and 86 amu TPD traces as two peaks about 230 and 265 K. No cyclohexene or benzene are detected in this case either.

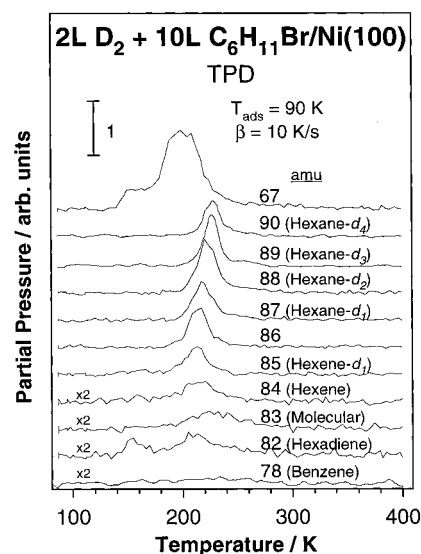


**Figure 7.** 67 (hexadiene and bromohexene), 90 (hexane- $d_4$ ), 89 (hexane- $d_3$ ), 88 (hexane- $d_2$ ), 87 (hexane- $d_1$  and hexene- $d_3$ ), 86 (hexene- $d_2$  and hexane- $d_0$ ), 85 (hexene- $d_1$ ), 84 (hexene), 83 (molecular desorption), 82 (hexadiene), and 78 (benzene) amu TPD from 2.0 langmuirs  $D_2 + 10.0$  langmuirs 6-bromo-1-hexene on Ni(100) at 90 K. These data show extensive H–D exchange on the 5-hexen-1-yl that forms upon C–Br bond scission of the parent molecule, indicating a facile interconversion among nickelacycloheptane, hexenyl, and hexadiene surface intermediates ( $L =$  langmuir).

The data from TPD experiments with a 2.0 langmuir deuterium (instead of hydrogen) pre-dose are presented in Figure 7. Extensive deuterium incorporation is seen in the results from this experiment. For one, at least five hexane isotopomers (with zero to four deuterium substitutions, 86 to 90 amu) display peaks in this TPD traces, with temperatures that increase from 220 K for hexane- $d_0$  to 228 K for hexane- $d_4$ . The amounts of hexane- $d_2$  and hexane- $d_3$  produced here are about equal, while the yields of hexane- $d_1$  and hexane- $d_4$  amount to only about one-half of that. The formation of hexanes up to hexane- $d_3$  can easily be explained by hydrogenation of 5-hexen-1-yl species at both the double bond and the carbon atom directly bound to the surface, but the formation of a significant amount of hexane- $d_4$  indicates that there must also be some hydrogen exchange between the hexenyl species and the coadsorbed deuterium on the surface. Normal hexene (84 amu), hexene- $d_1$  (85 amu), and hexene- $d_2$  (86 amu, together with hexane- $d_0$ ) were also detected. Large amounts of normal hydrogen desorb between 250 and 500 K (data not shown) although the surface is predosed with deuterium, indicating that most of the hydrocarbon species on the surface undergo total decomposition. Finally, significant signals are also seen in the HD and  $D_2$  traces around 330 and 480 K (also not shown), corroborating the extensive H–D exchange that must take place within the hydrocarbon surface moieties in this system.

Representative TPD data from studies with the most likely  $C_6H_{10}$  surface intermediates in the cyclization of 1,6-diiodohexane on Ni(100) are shown in Figure 8. Methylene cyclopentane, which appears to form via thermal activation of the diiodo compound around 240 K, mostly dehydrogenates completely to hydrogen and surface carbon. The left panel of Figure 8 shows the resulting TPD traces for  $H_2$  (with four peaks at 305, 360, 440, and 500 K), molecular desorption (at 155, 185, and 217 K), and methyl cyclopentane (a small feature at 155 K), from 4.0 langmuir of methylene cyclopentane on Ni(100). No  $C_6$ -cyclic products are formed in this case, no benzene in particular. Interestingly, a small amount of isomerization to 1-methyl-

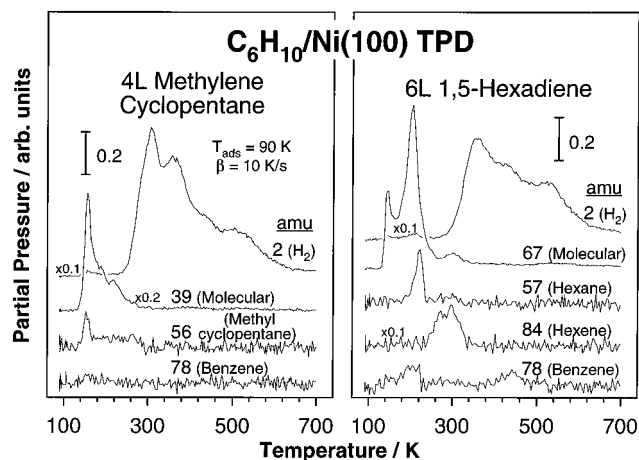


**Figure 8.** Left: 2 ( $\text{H}_2$ ), 39 (methylene cyclopentane), 56 (methyl cyclopentane), and 78 (benzene) amu TPD spectra from 4.0 langmuirs of methylene cyclopentane dosed on Ni(100) at 90 K. Right: 2 ( $\text{H}_2$ ), 67 (hexadiene), 57 (hexane), 84 (hexene), and 78 (benzene) amu TPD spectra from 6.0 langmuirs of 1,5-hexadiene dosed on Ni(100) at 90 K. Benzene is produced from the hexadiene but not from the  $\text{C}_5$ -cyclic molecule (L = langmuir).

cyclopentene occurs around 225 K, and extensive H–D exchange can be induced by deuterium coadsorption, but the discussion of those reactions is beyond the scope of this paper.<sup>21</sup> TPD experiments with both 1-methyl cyclopentene and methyl cyclopentane indicate that their molecular desorption occurs below 250 K and that neither compound leads to the formation of cyclohexane, cyclohexene, or benzene either (data not shown).

The hydrogen (2 amu), 1,5-hexadiene (67 amu), hexane (57 amu), hexene (84 amu), and benzene (78 amu) desorption traces from TPD experiments with 6.0 langmuirs of 1,5-hexadiene adsorbed on Ni(100) at 90 K are shown in the right panel of Figure 8. All the hydrogen produced in this case desorbs above 300 K in three main stages at approximately 355, 420, and 530 K. Molecular desorption of the diene is observed mostly at 145 (multilayer) and 205 (monolayer) K, but there is a third small peak around 300 K. A small fraction of the 1,5-hexadiene hydrogenates to hexene, as seen by the broad desorption peak in the 84 amu trace about 290 K, and an even smaller amount is completely hydrogenated to hexane at 220 K (the peak in the 57 amu trace). Of particular importance to the subject of this paper is the fact that a small but detectable amount of benzene evolves from this system as well in two peaks around 200 and 445 K.

Finally, Figure 9 compares the TPD results for the formation of benzene (left), cyclohexene (center), and cyclohexane (right) from 1,6-diiodohexane with those from various six-membered cyclic hydrocarbons adsorbed on Ni(100) at 90 K.<sup>22</sup> The intermediates considered here are cyclohexane, cyclohexyl (produced via the thermal activation of iodicyclohexane), and cyclohexene. Focusing first on the benzene TPD spectra, it can be seen from this figure (Figure 9, left panel) that only the cyclohexyl and cyclohexene surface species are capable of dehydrogenating to that product. Notice in particular that no benzene is produced by thermal activation of cyclohexane, presumably because the surface cannot activate the C–H bonds of that molecule before it desorbs molecularly. Two peaks are seen in the top two traces of the figure below 180 and around 450 K while only the low-temperature desorption state is seen in the case of 1,6-diiodohexane, but that is only a reflection of the different coverages of the surface species in each case; benzene itself desorbs molecularly from Ni(100) around 165 and 480 K, which, according to previous reports,<sup>23–25</sup> correspond

to desorption from tilted and flat-lying benzene adsorption states, respectively.

The middle panel of Figure 9 summarizes the TPD desorption profiles for the formation of cyclohexene from the same group of hydrocarbons. Cyclohexene molecular desorption is detected in two stages, at about 145 and 175 K, the same as in the case of the cyclohexene produced via the thermal conversion of adsorbed 1,6-diiodohexane. The activation of iodicyclohexane, which initially grafts cyclohexyl moieties on the surface, also yields cyclohexene, but only at about 175 K. On the other hand, no cyclohexene is observed after adsorption of cyclohexane, again suggesting that the need for the initial activation of a C–H bond limits the surface reactivity of that molecule.

Last, the cyclohexane TPD traces in the right panel of Figure 9 show that only cyclohexyl groups (from iodicyclohexane) are capable of hydrogenating to cyclohexane. The desorption temperature in that case is about 165 K, some 30 K lower than that from a surface directly dosed with the molecular species. The amounts of cyclohexane produced from chemisorbed cyclohexene or 1,6-diiodohexane are negligible.

#### 4. Discussion

The data reported in this paper provides some insight into the mechanism for hydrocarbon cyclization steps on nickel surfaces. Our previous temperature-programmed desorption (TPD) and X-ray photoelectron spectroscopy (XPS) studies with 1,3-diiodopropane and 1-chloro-3-iodopropane on Ni(100) had already shown that direct C–C coupling steps in metallacyclic intermediates are feasible on nickel surfaces. In particular, thermal activation of either compound yields some gas-phase cyclopentane, presumably after the formation of a nickel-acyclobutane intermediate.<sup>12</sup> This is somewhat puzzling, in particular because no direct evidence of coupling reactions has been seen between aliphatic alkyl groups on the same surface.<sup>6,11,26</sup> There is a report of  $\text{C}_2$ – $\text{C}_4$  hydrocarbon formation on Ni(100) following exposures of that surface to large amounts of methyl radicals,<sup>27</sup> but the mechanism for such a process is at present unknown. According to the results from the work reported here, 1,6-diiodohexane, like the dihalopropanes, reacts to yield some cyclic hydrocarbons, cyclohexene and benzene in particular, but, as it will be argued below, by following a mechanism other than direct C–C coupling.

To analyze the results from the experiments with 1,6-diiodohexane on Ni(100), we start from the knowledge acquired in our previous studies with mono- and diiodoalkanes on Ni(100).<sup>7–9,11,12,19,22,28–33</sup> As in other cases, the I 3d XPS data reported here show that the adsorption of 1,6-diiodohexane below 100 K is molecular. Furthermore, at low coverages, the diiodoalkane is likely to bond to the surface through both of its iodine atoms, but as the exposures are increased, the new molecules probably adsorb via one single iodine atom and stack in an approximately vertical orientation instead.<sup>12</sup>

Annealing the chemisorbed 1,6-diiodohexane to temperatures around 160 K leads to the dissociation of the C–I bonds that interact directly with the surface, a step that has an activation energy of only about 2–4 kcal/mol.<sup>11,19</sup> On the basis of the data obtained here it could not be conclusively determined whether both C–I bonds in the 1,6-diiodohexane break sequentially or simultaneously, but the TPD results suggest that both mechanisms may operate in this system. On one hand, some iodoalkane desorption is detected in TPD experiments for the intermediate to high initial coverages of 1,6-diiodohexane necessary to observe any products other than hydrogen. This indicates that at the very least some of the molecules undergo

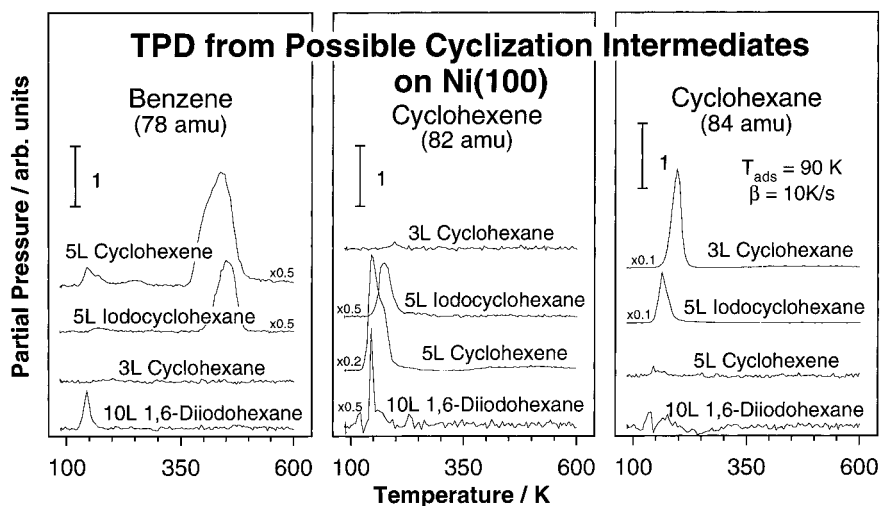


**Figure 9.** Benzene (78 amu, left panel), cyclohexene (82 amu, center), and cyclohexane (84 amu, right) TPD spectra from Ni(100) dosed with various C<sub>6</sub>-cyclic hydrocarbons (5.0 langmuirs cyclohexene, 5.0 langmuirs iodocyclohexene, and 3.0 langmuirs cyclohexene). The bottom traces are those for 10.0 langmuirs of 1,6-diiodohexane, the same as in Figure 1, and are reproduced here for reference. From the C<sub>6</sub>-cyclic molecules, only cyclohexene displays the relative yields for benzene, cyclohexene, and cyclohexane consistent with being an intermediate in the cyclization of 1,6-diiodohexane (L = langmuir).

one single C–I bond-scission step and then follow a reductive elimination reaction with surface hydrogen. This behavior has also been seen with dihalopropanes, and can be explained by the adsorption of some diiodo molecules in a standing-up position at high coverages.<sup>12</sup> In contrast, the formation of benzene and cyclohexene at temperatures well below 180 K suggests that other 1,6-diiodohexane molecules may suffer the simultaneous (or near simultaneous) breakage of both C–I bonds. The low temperature of the dissociation of the C–I bonds in a given molecule is supported by the results shown in Figure 9, which highlight the fact that the detection of either benzene or cyclohexene from 1,6-diiodohexane is not limited to any significant extent by the rate of the ring formation steps, since the desorption temperatures of those products are the same or lower than those for benzene or cyclohexene molecular desorption on Ni(100).

The breakage of both of the C–I bonds in the 1,6-diiodohexane molecules on Ni(100) must result at least in part in the formation of a metallacycle (nickelacycloheptane) species on the surface. The identification of that moiety was accomplished here indirectly via its titration with deuterium, by the detection of hexane-*d*<sub>2</sub> in the TPD experiment with D<sub>2</sub> and IC<sub>6</sub>H<sub>12</sub>I shown in Figure 4. This six-carbon metallacycle can follow a series of conversion steps upon further heating of the surface, including its hydrogenation to hexane, a hydrogenation–dehydrogenation sequence of steps to produce hexene, and its cyclization plus dehydrogenation to cyclohexene, methylene cyclopentane, and benzene. In this report, the focus is on the particular nature of the cyclization reactions. When the previous observation of cyclopropane formation from dihalopropane compounds,<sup>12</sup> the formation of C<sub>6</sub> ring compounds from 1,6-diiodohexane reported here, and the similar formation of C<sub>5</sub>-cyclic products from 1,5-diiodopentane are added together,<sup>21</sup> it could be said that the cyclization of metallacycles is a general reaction on Ni(100). However, unlike the products obtained with 1,6-diiodohexane, the three-carbon metallacycle generated from 1,3-diiodopropane leads to the sole desorption of cyclopropane, the saturated cyclic molecule; no cyclopropene is produced in that case at all. This closure of the C<sub>3</sub> rings was previously reported to involve the direct coupling of the two methylene groups directly attached to the surface. Even though C–C coupling steps are common in organometallic and organic

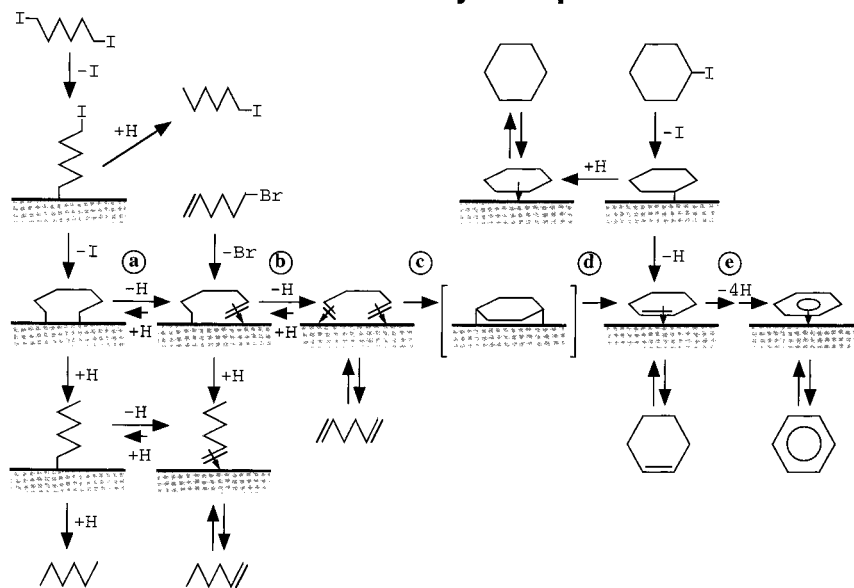
systems,<sup>26,34</sup> on surfaces it has only been directly observed over coinage (silver, copper, gold) metals;<sup>35,36</sup> no previous examples were available for such a reaction on nickel. As will be discussed below, we do not believe that the direct coupling of the end carbons in the metallacyclic species that results from activation of 1,*n*-diiodoalkanes is viable for molecules with more than four carbon atoms (*n* > 4) either, because no saturated cyclic compounds are produced in those cases at all.

The unraveling of the mechanism for the conversion of 1,6-diiodohexane on Ni(100) is hindered by the fact that most of the cyclization steps occur at quite low temperatures, below 150 K; the resulting cyclohexene and benzene both desorb about 140 K. As noted previously, these desorption temperatures are well below those for the molecular desorption of either cyclohexene or benzene from Ni(100), which are 180 K (cyclohexene monolayer) and 165 K (benzene tilted species), respectively. Furthermore, both cyclohexene and benzene formation involve a series of dehydrogenation steps on top of the required C–C bond formation reaction. The determination of the sequence in which those steps take place is at the heart of the understanding of the cyclization mechanism. Clearly, at least one dehydrogenation step precedes the formation of the C–C bond, otherwise the main product from the direct reductive elimination of nickelacycloheptane would be cyclohexane (see above). This is not surprising since early dehydrogenation reactions are common in alkyl species, via  $\beta$ -hydride elimination steps when possible.<sup>6,26,37,38</sup> In the case of metallacyclic intermediates, the question then centers around the number of dehydrogenation steps (either one or two, at one or both ends of the moiety) that precedes the closing of the ring. Below, we discuss this issue in terms of the steps depicted in Scheme 1.

To address the issue of the priority of dehydrogenation versus cyclization steps, we start by pointing out that, in the TPD experiments with 6-bromo-1-hexene, the resulting 5-hexen-1-yl species does not subsequently close on the Ni(100) surface. Notice that 5-hexen-1-yl is the moiety that would result from a single  $\beta$ -hydride elimination from nickelacycloheptane (step a in Scheme 1) and that its formation in the case of the activation of 1,6-diiodohexane is supported by the fact that deuterium coadsorption does facilitate its hydrogenation to hexene-*d*<sub>1</sub> (Figure 4). The lack of cyclization from 6-bromo-1-hexene could therefore be associated with the relatively high temperatures at

SCHEME 1

### Proposed Mechanism for the Cyclization of Nickelacycloheptane



which the hexenyl intermediate is formed in that case, since the C–Br bond only breaks around 200 K; the production of cyclohexene and benzene from 1,6-diiodohexane is over by 140 K. What is clear from the bromohexene experiments is the fact that 5-hexen-1-yl can be converted easily and reversibly into at least one second species that facilitates the H–D exchange reactions manifested by the results shown in Figure 7. It could be argued that H–D exchange in hexenyl moieties proceeds via the initial partial hydrogenation (deuterium) of the double bond (reverse of step a), but that would lead to the formation of a nickelacycloheptane intermediate, and the experiments with 1,6-diiodohexane have shown that once such a species is formed it then produces cyclohexene and benzene; none of that was seen in the case of 6-bromo-1-hexene. More likely, the hexenyl moiety exchanges its hydrogens via a  $\beta$ -hydride elimination in the alkyl side (step b) followed by hydrogen (deuterium) incorporation to the resulting double bond (reverse of step b); 1,5-hexadiene is expected to form on the surface in that case, a product that is actually detected in the TPD experiments (Figure 6). It is important to point out, however, that both hydrogenation and dehydrogenation reactions do occur with the hexenyl intermediate, since all hexane, hexene, and hexadiene are detected in TPD experiments with the bromohexene precursor; it is only the relative rates of those steps at the temperature where C–Br bond scission occurs that determines the selectivity toward hexadiene vs nickelacycloheptane formation. Also, H–D exchange via the activation of the allylic hydrogens cannot be ruled out in this case<sup>21</sup>

The alternative to 5-hexen-1-yl as the intermediate for the conversion of nickelacycloheptane to cyclic hydrocarbons is a continuing fast dehydrogenation of the hexenyl to 1,5-hexadiene (step b). Interestingly, the TPD experiments with hexadiene do show the production of detectable amounts of benzene; that was not the case with 6-bromo-1-hexene. These results provide direct evidence for a diene, not an alkenyl, as the source of C<sub>6</sub>-cyclic compounds in the case of the conversion of 1,6-diiodohexane. Again, the possibility of hexadiene hydrogenating to 5-hexen-1-yl (reverse of step b) prior to cyclization (step c) is ruled out by the fact that (1) the hexenyl itself, as prepared by using 6-bromo-1-hexene, does not produce any benzene, and, more

importantly, (2) the first cyclic intermediate that desorbs from the surface is cyclohexene. Double bond insertion into the nickel–carbon bond of a hexenyl intermediate would lead to the formation of a cyclohexyl moiety, and that species hydrogenates easily to cyclohexane; no cyclohexane was detected in any of the 1,6-diiodohexane, 6-bromo-1-hexene, or hexadiene TPD experiments. Figure 9 shows that cyclohexane and cyclohexyl both produce too much cyclohexane and not enough cyclohexene or benzene as compare to the acyclic C<sub>6</sub> hydrocarbons tested in this work to explain the chemistry of the diiodohexane. Only cyclohexene shows the right balance between those reactions.

We are left with the problem of explaining how the C–C bond formation actually takes place. Direct C–C coupling from nickelacycloheptane was ruled out early on because no cyclohexane is produced in the 1,6-diiodohexane TPD experiments. Also, although the insertion of double bonds into metal–carbon bonds is quite common in inorganic complexes,<sup>26,34</sup> such a step was also discarded here by the arguments presented in the previous paragraphs. Incidentally, TPD experiments with a mixture of iodomethane and ethylene on Ni(100) do not lead to the production of any C<sub>3</sub> hydrocarbon products (results not shown), indicating that double-bond insertion is in general not favorable on nickel surfaces, at least under vacuum. The data presented in this paper suggests the addition of two double bonds, those at the end of the hexadiene, instead. Unfortunately, there is to the best of our knowledge no precedent for this. We propose a half Diels–Alder (or 2 + 2 cycloaddition) reaction<sup>39</sup> leading to the formation of a 1,4-dicyclohexyl (step c) followed by isomerization/hydrogen migration to cyclohexene (step d). Benzene is produced via further dehydrogenation of this cyclohexene (step e).

Finally, there is a small production of methylene cyclopentane in the TPD experiments with 1,6-diiodohexane. Following the ideas presented above, it could be conceived that a fraction of the 1,6-hexadiene follows the same half Diels–Alder step as that in the formation of cyclohexene, but with one of the double bonds inverted so the C–C bond is formed between the first and fifth (not sixth) carbons. The end result in this case would be the dialkyl moiety that results from removing hydrogens from

the methyl and the cyclic C<sub>5</sub> carbons in methyl cyclopentane; isomerization of that species would yield methylene cyclopentane. The low yield of this pathway is easily understood on steric grounds.

It is interesting to put the results from this work in perspective in terms of the catalytic conversion of hydrocarbons on transition metals. Certainly, nickel is not known for its activity toward cyclization reactions because it usually promotes dehydrogenation and cracking processes instead. Nevertheless, studies on the catalytic conversion of *n*-hexane over nickel films indicate that the production of C<sub>6</sub> molecules displays a high selectivity toward cyclohexene and benzene formation.<sup>40</sup> Our results reproduce that observation quite nicely. In any case, most reforming catalysts are based on platinum, which is known to facilitate not only ring formation but also isomerization steps.<sup>1,5,41</sup> In terms of the mechanism for cyclization and aromatization reactions, the proposal that they may occur via the initial formation of C<sub>5</sub>-cyclic intermediates followed by ring expansion<sup>42</sup> was refuted in the past by results from isotopic labeling experiments.<sup>43</sup> Further experiments also showed that the changes in activity for aromatization as a function of surface structure are quite different from those for reactions involving C<sub>5</sub>-cyclic intermediates (such as the formation of C<sub>5</sub> cyclic products or isomerization), implying different mechanistic pathways for each.<sup>44</sup> This again is in entire agreement with our results (none of the C<sub>5</sub>-cyclic intermediates studied here, methyl cyclopentane, methylene cyclopentane, or 1-methyl-cyclopentane, led to the formation of any C<sub>6</sub>-cyclic products). Instead, the catalytic literature appears to have settled on the proposal of a triene intermediate leading to the formation of a cyclohexadiene followed by its dehydrogenation to the aromatic final product.<sup>45–47</sup> This is inconsistent with our observations on the chemistry of C<sub>6</sub> compounds on Ni(100), because cyclohexadienes are quite difficult to hydrogenate back to cyclohexene; our previous TPD experiments with both 1,3- and 1,4-cyclohexadienes proved that those molecules only dehydrogenate to benzene.<sup>22</sup> We cannot, however, completely rule out the possibility of a hexatriene–cyclohexadiene–cyclohexene sequence in the 1,6-diiodohexane/Ni(100) system studied here, since TPD data from surfaces where hydrogen is coadsorbed with 1,3-cyclohexadiene does yield a small amount of cyclohexene below 200 K.<sup>22</sup> Nevertheless, we still favor the mechanism involving the cyclization of hexadiene to cyclohexene. Such a mechanism cannot be discarded by the data from the catalytic work published to date, and has in fact been suggested in one publication based on the efficient way in which hexadienes also produce cyclohexenes.<sup>48</sup>

## 5. Conclusions

In this report, we have shown that the thermal decomposition of 1,6-diiodopropane on Ni(100) surfaces yields iodohexane, hexane, cyclohexene, methylene cyclopentane, and benzene. The initial dissociation of the C–I bonds is presumed to lead to the formation of a metallacycle on the surface. Cyclization of that species leads to the production of cyclohexene and to its subsequent dehydrogenation to benzene. Neither 5-hexen-1-yl species (from decomposition of 6-bromo-1-hexene) nor any of the suspected C<sub>5</sub> compounds (methyl cyclopentane, methylene cyclopentane, or 1-methyl-1-cyclopentene) are intermediates in this reaction sequence, because thermal activation of the corresponding compounds on the same Ni(100) surface does not yield any C<sub>6</sub>-cyclic product at all. Multiple β-hydride and reductive elimination steps allow for the interconversion of the initial nickelacycloheptane moiety to 5-hexen-1-yl and 1,5-

hexadiene species, which can then be hydrogenated to hexane and hexene, but only the hexadiene appears to be capable of undergoing a C–C bond-forming reaction to close the ring and yield cyclohexene.

**Acknowledgment.** Financial support for this research was provided by a grant from the National Science Foundation (CHE-9530191).

## References and Notes

- (1) Gates, B. C.; Katzer, J. R.; Schuit, G. C. A. *Chemistry of Catalytic Processes*; McGraw-Hill: New York, 1979.
- (2) Davis, S. M.; Somorjai, G. A. In *The Chemical Physics of Solid Surfaces and Heterogeneous Catalysis*; King, D. A., Woodhuff, D. P., Eds.; Elsevier: Amsterdam, 1982; Vol. 4 (Fundamental Studies of Heterogeneous Catalysis), p 217.
- (3) Zaera, F.; Somorjai, G. A. In *Hydrogen Effects in Catalysis: Fundamentals and Practical Applications*; Paál, Z., Menon, P. G., Eds.; Marcel Dekker: New York, 1988; p 425.
- (4) Zaera, F.; Tjandra, S.; Janssens, T. V. W. *Langmuir* **1998**, *14*, 1320.
- (5) Zaera, F. *Isr. J. Chem.*, in press.
- (6) Zaera, F. *Acc. Chem. Res.* **1992**, *25*, 260.
- (7) Tjandra, S.; Zaera, F. *Langmuir* **1992**, *8*, 2090.
- (8) Tjandra, S.; Zaera, F. *Surf. Sci.* **1993**, *289*, 255.
- (9) Tjandra, S.; Zaera, F. *Langmuir* **1994**, *10*, 2640.
- (10) Tjandra, S.; Zaera, F. *J. Catal.* **1994**, *147*, 598.
- (11) Tjandra, S.; Zaera, F. *J. Am. Chem. Soc.* **1995**, *117*, 9749.
- (12) Tjandra, S.; Zaera, F. *J. Phys. Chem. B* **1997**, *101*, 1006.
- (13) Pines, H. *The Chemistry of Catalytic Hydrocarbon Conversions*; Academic Press: New York, 1981.
- (14) Zaera, F. *Surf. Sci.* **1989**, *219*, 453.
- (15) Tjandra, S.; Zaera, F. *Langmuir* **1991**, *7*, 1432.
- (16) Gleason, N. R.; Zaera, F. *Surf. Sci.* **1997**, *385*, 294.
- (17) Zaera, F. *J. Phys. Chem.* **1990**, *94*, 5090.
- (18) Loaiza, A.; Xu, M.; Zaera, F. *J. Catal.* **1996**, *159*, 127.
- (19) Tjandra, S.; Zaera, F. *J. Vac. Sci. Technol.* **1992**, *A10*, 404.
- (20) Redhead, P. A. *Vacuum* **1962**, *12*, 203.
- (21) Tjandra, S.; Zaera, F. To be published.
- (22) Tjandra, S.; Zaera, F. *J. Catal.* **1996**, *164*, 82.
- (23) Myer, A. K.; Schoofs, G. R.; Benziger, J. B. *J. Phys. Chem.* **1987**, *91*, 2230.
- (24) Netzer, F. P.; Rangelov, G.; Rosina, G.; Saalfeld, H. B.; Neumann, M.; Lloyd, D. R. *Phys. Rev. B* **1988**, *37*, 10399.
- (25) Hoffmann, H.; Zaera, F.; Ormerod, R. M.; Lambert, R. M.; Wang, L. P.; Tysse, W. T. *Surf. Sci.* **1990**, *232*, 259.
- (26) Zaera, F. *Chem. Rev.* **1995**, *95*, 2651.
- (27) Dickens, K. A.; Stair, P. C. *Langmuir* **1998**, *14*, 1444.
- (28) Tjandra, S.; Zaera, F. *J. Am. Chem. Soc.* **1992**, *114*, 10645.
- (29) Tjandra, S.; Zaera, F. *J. Catal.* **1993**, *144*, 361.
- (30) Tjandra, S.; Zaera, F. *Langmuir* **1993**, *9*, 880.
- (31) Tjandra, S.; Zaera, F. *Surf. Sci.* **1995**, *322*, 140.
- (32) Zaera, F.; Tjandra, S. *J. Am. Chem. Soc.* **1996**, *50*, 12738.
- (33) Gleason, N. R.; Zaera, F. *J. Catal.* **1997**, *169*, 365.
- (34) Collman, J. P.; Hegedus, L. S.; Norton, J. R.; Finke, R. G. *Principles and Applications of Organotransition Metal Chemistry*; University Science Books: Mill Valley, 1987.
- (35) Zhou, X.-L.; White, J. M. *J. Phys. Chem.* **1991**, *95*, 5575.
- (36) Bent, B. E. *Chem. Rev.* **1996**, *96*, 1361.
- (37) Zaera, F. *J. Am. Chem. Soc.* **1989**, *111*, 8744.
- (38) Zaera, F.; Bernstein, N. *J. Am. Chem. Soc.* **1994**, *116*, 4881.
- (39) March, J. *Advanced Organic Chemistry: Reactions, Mechanisms, and Structure*; McGraw-Hill: Tokyo, 1968.
- (40) Anderson, J. R.; Macdonald, R. J.; Shimoyama, Y. *J. Catal.* **1971**, *20*, 147.
- (41) Anderson, J. R. *Adv. Catal.* **1973**, *23*, 1.
- (42) Garin, F.; Gault, F. G. *J. Am. Chem. Soc.* **1975**, *97*, 4466.
- (43) Dautzenberg, F. M.; Platteeuw, J. C. *J. Catal.* **1970**, *19*, 41.
- (44) Davis, S. M.; Zaera, F.; Somorjai, G. A. *J. Catal.* **1984**, *85*, 206.
- (45) Paál, Z.; Tétényi, P. *J. Catal.* **1973**, *30*, 350.
- (46) Pines, H.; Nogueira, L. *J. Catal.* **1981**, *70*, 391.
- (47) Paál, Z. In *Catalytic Naphta Reforming: Science and Technology*; Antos, G. J., Aitani, A. M., Parera, J. M., Eds.; Marcel Dekker: New York, 1995; p 19.
- (48) Zimmer, H.; Rozanov, V. V.; Sklyarov, A. V.; Paál, Z. *Appl. Catal.* **1982**, *2*, 51.